First International Conference on Damage Tolerance of Aircraft Structures
R. Benedictus, J. Schijve, R.C. Alderliesten, J.J. Homan (Eds.)

COMPARISON OF DIFFERENT SET-UPS FOR FATIGUE TESTING OF THIN COMPOSITE LAMINATES IN BENDING

I. De Baere*, W. Van Paepegem* and J. Degrieck*

* Department of Mechanical Construction and Production, Faculty of Engineering, Ghent University.
Sint-Pietersnieuwstraat 41, B-9000 Gent, Belgium.

e-mail: Ives.DeBaere@UGent.be

Abstract: *After developing a fatigue damage model, validation of this model is a necessity. This validation should preferably be done under fatigue loading conditions which are different from the ones used for the development of the model.*
This study investigates whether a special design of a bending set-up is suited for the fatigue testing of thin fibre-reinforced composites with a low bending stiffness and the validation of fatigue damage models, developed in uni-axial loading conditions. First, the disadvantages of a three-point bending set-up for thin laminates are commented on. Then, a four-point bending set-up is discussed, because of its interesting finite-element model. Clamped supports are added to decrease the midspan displacement. This is followed by the discussion of the clamped three-point bending set-up. It may be concluded that the clamped three-point bending set-up is very promising for experimental work, since it increases the measured loads and decreases the midspan displacement with respect to the regular three-point bending set-up, although further modification of the set-up is necessary to avoid slipping in the grips.
The material used for this study was a carbon fabric-reinforced polyphenylene sulphide.

1 INTRODUCTION

The vast majority of fatigue tests on fibre-reinforced composites is performed in uni-axial tension/tension or tension/compression fatigue [1-5]. These tests are accepted by international standards (ASTM D3479) and provide the S-N data for the tested material.

Although bending fatigue tests are not widely accepted as a standard, they are used a lot for research purposes [6-8] and they do have some important advantages: (i) bending loads often occur in in-service loading conditions, (ii) there are no problems with buckling, compared to tension/compression fatigue, and (iii) the required forces are much smaller. To evaluate the stiffness degradation and damage growth in the fibre-reinforced laminate, the hysteresis loop of one loading cycle can be measured. In case of three-point bending fatigue, the history of bending force versus midspan displacement is recorded.

In [9], the authors examined a standard three-point bending set-up for fatigue testing of thin composite laminates. It was concluded that this set-up was not suited because of the following three reasons: (i) due to the specimen's low bending stiffness, the midspan displacement of the specimen was very large, limiting the test frequency in the fatigue test, (ii) the apparent hysteresis seen in the force-displacement curves was entirely due to friction in the large relative sliding movement between the specimen and the outer roller supports, and (iii) the computational demand for the finite element simulations was very large, because modelling of geometric nonlinearity and friction at the supports had to be taken into account.

This study investigates whether a modified bending set-up may be used for the validation of fatigue damage models. First, the disadvantages of a modified three point-bending set-up with rotating supports are commented on. Then, a four-point bending set-up is discussed, because its loading conditions allow easy finite-element modelling. A clamped four-point bending set-up is then discussed, since the clamping would reduce the midspan displacements. This is followed by a clamped three-point bending set-up. Finally, some conclusions are drawn. In the next paragraph, the used composite material and tensile machine are discussed.

2 MATERIALS AND METHODS

2.1 Composite Material

The material used for the experiments was a 5-harness satin-weave carbon fabric-reinforced polyphenylene sulphide (PPS). The carbon PPS plates were hot pressed, one stacking sequence was used for this study, namely $[(0^o,90^o)]_{2s}$ where $(0^o,90^o)$ represents one layer of fabric. The in-plane elastic properties and the tensile strength properties are listed in Table 1. This material was supplied to us by Ten Cate Advanced Composites.

E_{11} [GPa]	56.0	X_T [MPa]	736
E_{22} [GPa]	57.0	ε_{11}^{ult} [-]	0.011
ν_{12} [-]	0.033	Y_T [MPa]	754.0
G_{12} [GPa]	4.175	ε_{22}^{ult} [-]	0.013
		S_T [MPa]	110.0

Table 1 : Elastic and strength properties of the CETEX® material.

2.2 Equipment

All bending tests were performed on an INSTRON 1342 servo-hydraulic machine with a FastTrack 8800 digital controller. For the registration of the data, a combination of a National Instruments DAQpad 6052E for fireWire, IEEE 1394 and SCB-68 pin shielded connecter were used. The load and displacement were sampled on the same time basis.

3 EXPERIMENTS AND DISCUSSION

3.1 The modified three-point bending set-up with rotating supports

In [10], the authors had already examined whether the standard three-point bending set-up could be improved for testing thin composite laminates. A special set-up with rotating outer supports was presented (Figure 1 (a)), to reduce the effect of friction at the outer supports, and to allow for fully-reversed bending fatigue tests. However, two major problems remained: (i) the midspan displacements were still too large, limiting the test frequency of the fatigue test, and (ii) the finite element modelling of the set-up was still very cumbersome, because the (rotating) supports needed to be modelled to correctly calculate the bending force and displacements (Figure 1 (b)).

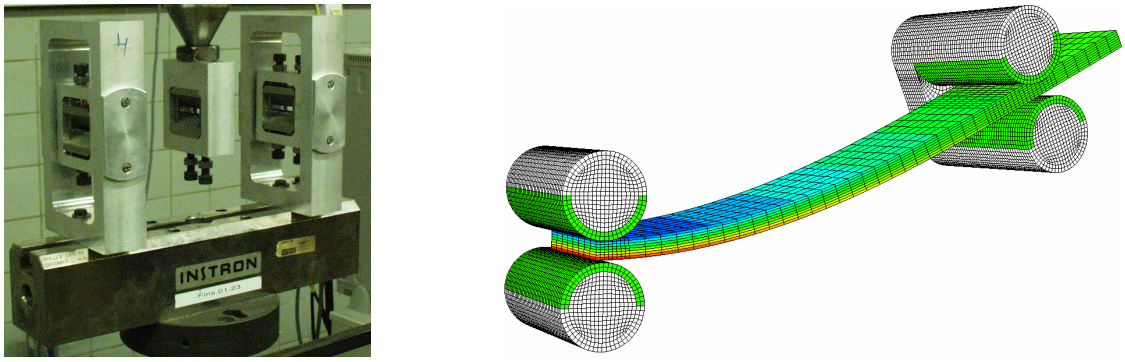

(a) the actual set-up (b) Illustration of the finite-element simulation

Figure 1 : The modified three-point bending set-up with rotating supports [10].

3.2 The four-point bending set-up

Contrary to the three-point bending set-up presented in the previous paragraph, a four-point bending set-up has a more interesting load distribution for modelling (Figure 2).

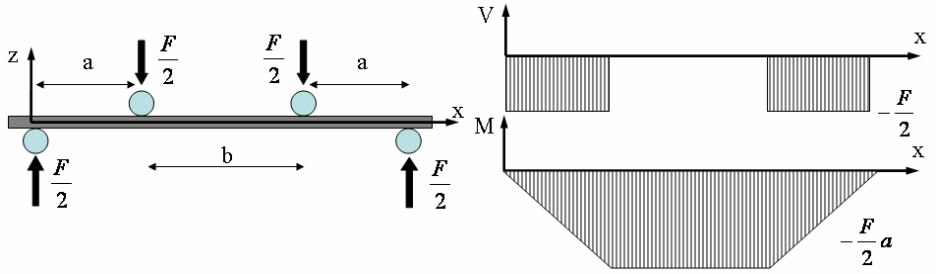

Figure 2 Illustration of the occurring loads in a four-point bending set-up.

The area between the two indenting rolls has a constant bending moment equal to –F/2 × a and no transverse force. As a result, the finite-element modelling of a load controlled test is very straightforward, only the section between the two indenting rolls must be modelled and a corresponding moment must be applied.

Figure 3 (a) shows the used geometry for these experiments.

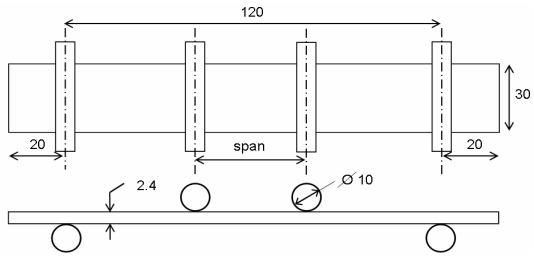

(a) Dimensions of the used four-point bending coupon in millimetres.

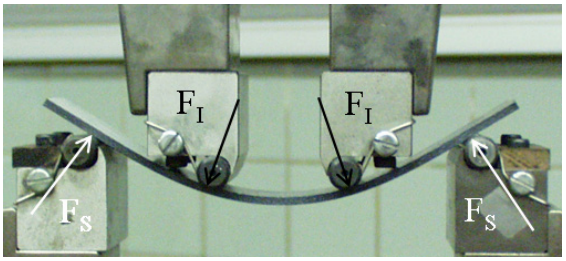

(b) Illustration of the problems with the four-point bending set-up

Figure 3 : Four-point bending set-up.

Figure 3(b) shows the major set back of this set-up. The low bending stiffness of the specimens leads again to very large midspan displacements, so that the occurring loads are no longer given by Figure 2. Since F_S and F_I are perpendicular to the (bent) surface of the specimen, they are no longer vertical, introducing normal forces in the specimen. Therefore, the simple finite element model described above is no longer valid and the entire set-up must be modelled and a geometrically non-linear calculation must be performed. As a result, the main advantage of this set-up over the standard three-point bending, namely the straight-forward numerical modelling, is lost because the midspan displacement of the thin laminates under study is too large.

Moreover, friction comes into play again. Several loading and unloading experiments were done with a varying span between the load striking edges of 30, 40 and 50 mm respectively. The force-displacement curves for the three set-ups are shown in Figure 4 (a). It must be noticed that, even for the 30 mm span, the loads are relatively low and the midspan displacements are quite high, again limiting the maximum frequency of a fatigue test. Quite large hysteresis loops are visible, but very limited permanent deformation is visible. The hysteresis loops however, are entirely due to the friction on the supports, as was documented in [9]. This can be seen in the evolution of the force as a function of time in Figure 4 (b), where the sudden drop in force becomes visible.

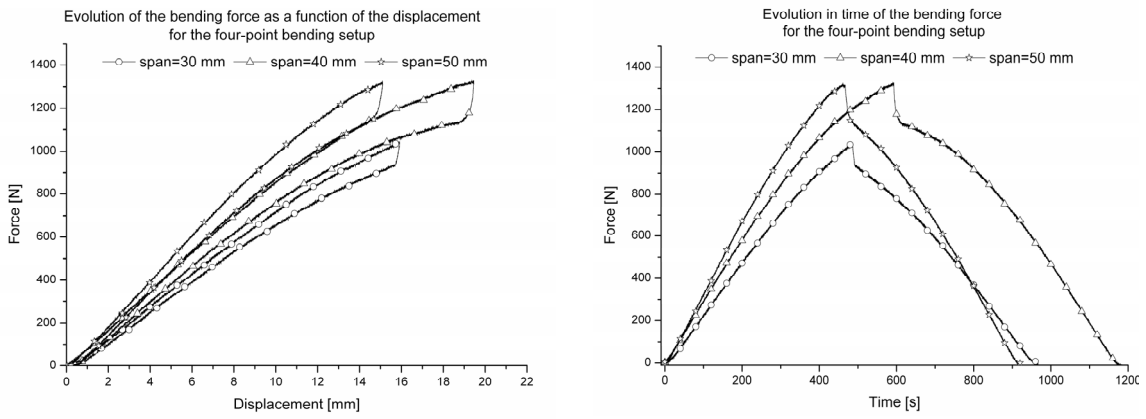

(a) Force-displacement curves

(b) Force-time curves

Figure 4 : Hysteresis loops in the four-point bending experiments.

3.3 The clamped four-point bending set-up

The next step is to consider a four-point bending set-up, where the ends of the specimen are clamped, instead of simply supported. Although this set-up is statically indeterminate, the elastic properties do not come into play in the formulas for the reaction forces and moments, because the imposed slope at the clamped ends is zero.

Unfortunately linear beam theory predicts that failure should always occur at the clamped ends. Indeed, the bending moment at the clamps, using the dimensions from Figure 2, is given by [12]:

$$M = F\frac{l^2 - b^2}{4l} \tag{1}$$

Where l equals a+b. The moment in the area between the indenters is given by [12]:

$$M^* = F\frac{(l-b)^2}{4l} \tag{2}$$

Solving $M^* > M$ yields $b > l$, which of course is impossible.

One experiment was done to see if the geometric nonlinearity, which induces membrane stresses, could alter this condition, but the specimen failed indeed at the clamped end. However, the experiment yielded a higher bending load for a lower midspan displacement; the specimen failed at 2636 N with corresponding midspan displacement of 8.3 mm.

3.4 The clamped three-point bending set-up

Because of the promising results of the clamped edges in the previous paragraph, the same principle is applied to a three-point bending set-up. The used set-up is illustrated in Figure 5 (a), the dimensions of the coupons used for these bending experiments are shown in Figure 5 (b), all dimensions are in millimetres.

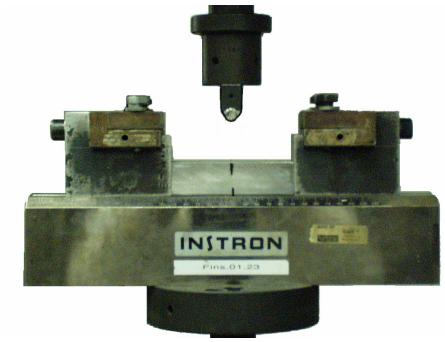

(a) The clamped three-point bending set-up with anti-sliding block

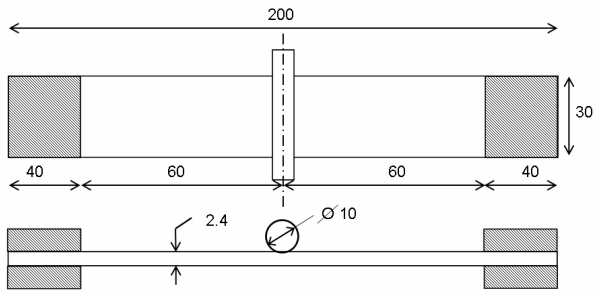

(b) Dimensions of bending coupon in millimetres

Figure 5 : The clamped three-point bending set-up.

The results of a few quasi-static tests are shown in Figure 6, the corresponding displacement speed was 2 mm/min. It may be remarked that the results are very reproducible, there is only a limited difference, due to scatter on the results. Furthermore, high forces for low displacements are achieved; the loads are four times higher at failure, for less than half the displacement when compared with the standard three-point bending set-up [10].

The two grips which clamp the specimen's ends, are mounted on a supporting steel fixture with a T-sleeve connection. Preliminary tests had shown that the two clamps can slide towards each other during the test, even if the maximum torque is applied on the bolts that clamp the grips on the supporting fixture. Therefore, a massive block of aluminium was placed between the two grips, at the exact width, preventing them from sliding inwards, as shown in Figure 5 (a). This observation indicates however that the induced membrane stresses due to geometric nonlinearity, must be very large.

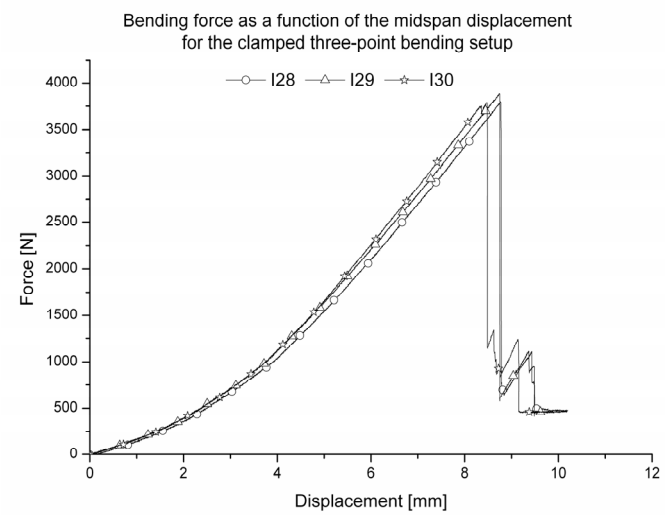

Figure 6 : Force-displacement curves of the quasi-static test with the clamped three-point bending set-up.

To investigate in which relative proportion the membrane stresses and bending stresses contribute to the resultant bending force, finite-element simulations have been done using ABAQUS™ Standard. Further, the set-up was modelled both with 3D continuum elements and 1D beam elements, to investigate if a much faster 1D model could accurately describe the stress state in the specimen. Both models are shown in Figure 7. Figure 7(a) shows the 3D model. Using the symmetry of the set-up, only a quarter was modelled in 3D quadratic brick elements with reduced integration, C3D20R; the size of the elements was 1 mm to have a dense mesh. In a first simulation, the gripped section of the specimen was not allowed to move inwards (3D clamped). In a second simulation, the gripped section could slide freely (3D Sliding). The boundary conditions for these simulations are given in Table 2; since 3D elements are used, there are no rotational degrees of freedom. For the bending load, a displacement $U_2 = 10$ mm was enforced on the reference point of the indenting roll, R_P.

Simulation	Face A	Face B	Face C	Face D
3D clamped	$U_1 = 0$	$U_2 = 0$	$U_1 = U_2 = 0$	$U_1 = U_2 = U_3 = 0$
3D sliding	$U_1 = 0$	$U_2 = 0$	$U_2 = 0$	$U_2 = U_3 = 0$

Table 2 : Used boundary conditions for the three-dimensional simulations.

Figure 7(b) shows the 1D finite element model. For this simulation, no symmetry was used, so the entire specimen was modelled, using a 3 node quadratic beam element in space, B32 with a size of 2 mm. For points A and C, all movement was restricted, which means that $U_1 = U_2 = U_3 = 0$; $\alpha_1 = \alpha_2 = \alpha_3 = 0$; a vertical displacement $U_2 = 10$ mm was enforced on point B. As for the 3D case, a 1D clamped and a 1D sliding simulation were done.

Of course, for both the 3D and 1D simulation, a geometrically nonlinear analysis was performed. The implemented material data are the same as in Table 1.

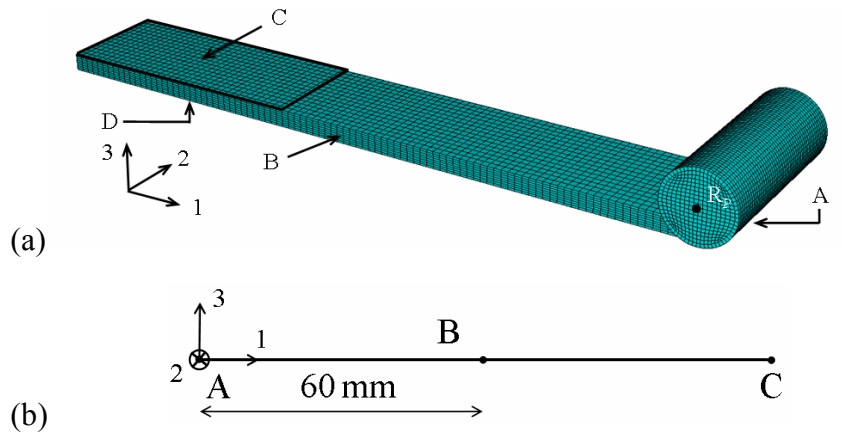

Figure 7 : (a) 3D finite element model of the clamped three-point bending set-up (with symmetry); (b) 1D finite element model of the clamped set-up (without symmetry).

From the 1D model, it is very easy to obtain values of the bending moments, longitudinal and transverse forces for both the clamped and sliding calculation, whereas for the 3D simulations, these values need to be calculated manually from the stress distributions. Figure 8 gives an overview of the values of the bending moment, the transverse force and the longitudinal force for the clamped set-up (Figure 8(a)) and the sliding set-up (Figure 8(b)), for a displacement of 9 mm, corresponding to final fracture in the static experiments. The forces have been rescaled to have a clear image; the scaling factor differs for both graphs.

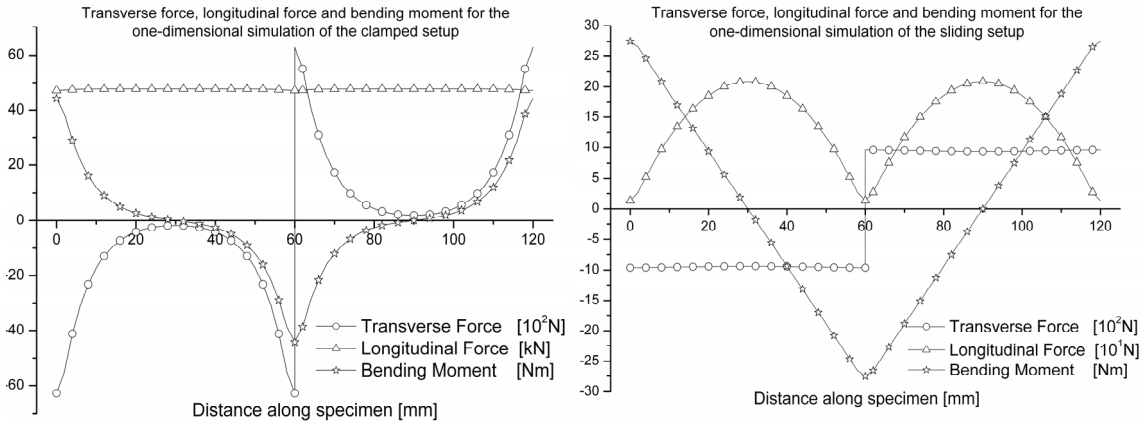

(a) Clamped set-up (b) Sliding set-up

Figure 8 : Evolution of the longitudinal force, transverse force and bending moment along the specimen.

Because of the clamping, very high longitudinal forces are imposed. For the sliding set-up, the longitudinal force only becomes 200 N, whereas for the clamped specimen, the force is almost 47800 N, which is almost 250 times higher. For the sliding set-up, the evolution of the bending moment and transverse force is about the same as for the standard three-point bending set-up. By preventing the ends of the specimen from sliding inwards, the maximum

bending moment almost doubles, whereas the transverse force in the centre of the specimen increases from 962 N to 6280 N. In Figure 9, the evolution of the longitudinal stress across the height of the specimen is compared for both the 1D and 3D analysis in the centre of the specimen at the same corresponding midspan displacement. It must be remarked that there is an excellent correspondence, except near the top of the specimen, where the 3D analysis predicts a higher compressive stress than the 1D analysis. This is probably due to the local indentation of the load striking edge which is modelled in the 3D analysis. This again proves that the one-dimensional simulation is very useful for the validation of fatigue damage models, since there is only a limited deviation in the longitudinal stresses.

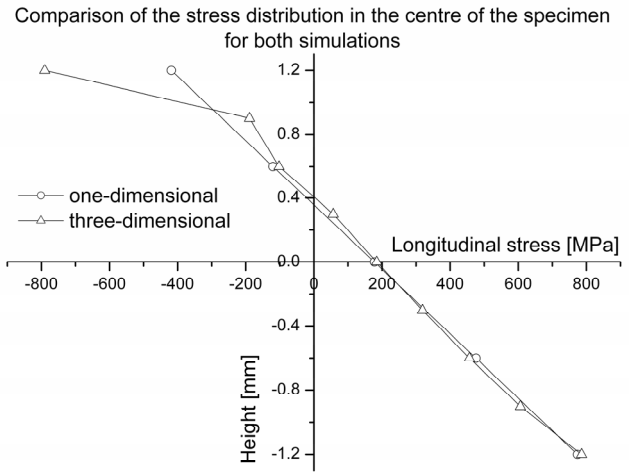

Figure 9 : Height distribution of the longitudinal stress in the centre of the specimen.

Finally, the force-displacement curves calculated from the 3D and 1D analysis are compared with the experimental results from the static tests (see Figure 6). The results are shown in Figure 10(a). First of all, it must be noted that if sliding in the grips is allowed, the force decreases significantly for a given displacement. It can also be remarked that the prediction of the simple elastic beam theory corresponds very well with the 3D analysis. This is very interesting for fatigue simulations with damage models, since a one-dimensional calculation is done in a matter of seconds, whereas the three-dimensional analysis takes a few hours to complete because of the dense mesh needed for accurate results.

Unfortunately, the experimental curve from the static test I28 lies in between the two extremes (clamped and sliding), so this indicates that little sliding must be present in the experiments. Nevertheless, because of the promising results in the quasi-static tests, some fatigue tests have been done. During those tests, it was noticed that after a few hundred cycles, the indenter lost contact over a certain period of time during every loading cycle. This is illustrated in Figure 10(b), which shows the evolution of the bending force and the displacement as a function of time for a few cycles from a displacement-controlled test with amplitude of 6 mm and a frequency of 2 Hz.

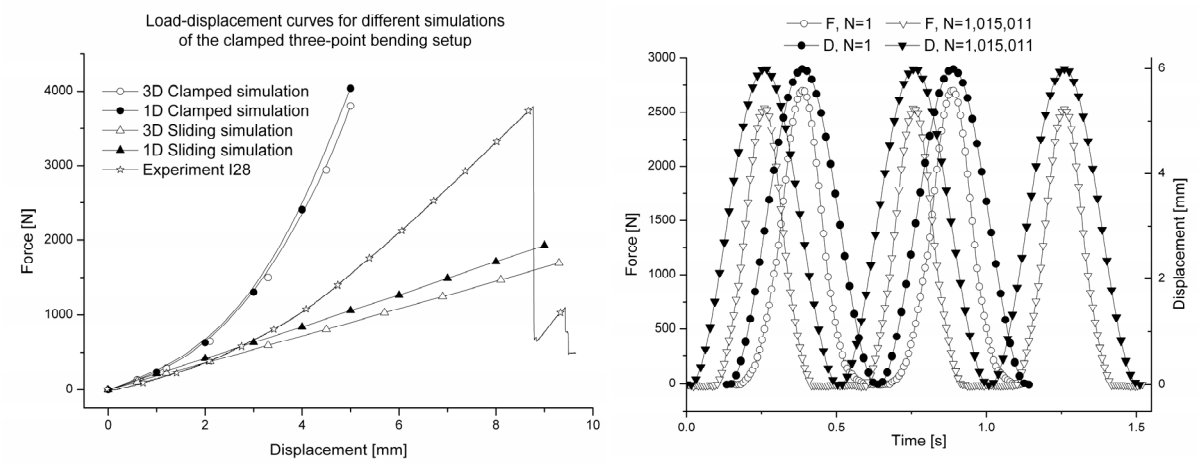

(a) (b)

Figure 10 : (a) Force-displacement curves of the quasi-static test with the clamped three-point bending set-up; (b) Force and displacement as a function of time for the first and last measurement.

For the last depicted cycle (N = 1,015,011 cycles) the load F remains zero for a certain period of time, although the displacement D varies. This means that the indenter looses contact during cycling. The latter may be caused by permanent deformation or slipping inside the grips. Therefore, small markings were placed on the specimen next to the clamps to verify if the specimen slips out of the grips. It was noticed that the specimen indeed slipped over a very limited distance, circa 0.5 mm, because of the very high membrane stresses. This would explain the loss of contact in Figure 10(b), although permanent deformation may not be neglected. Therefore, extra precautions must be developed to avoid this sliding. Possibilities are to use an additional actuator to compensate the gripping or to use bolts through the specimen, ensuring that this does not advance preliminary failure.

Further efforts are undertaken now to optimize this clamped three-point bending set-up for fatigue testing of thin composite laminates with a low bending stiffness.

4 CONCLUSIONS

Different bending set-ups have been discussed for the testing of thin composite laminates. A four-point bending set-up has the advantage of being very easily modelled, but the experiments yield low bending forces for large midspan displacements, which only allow low testing frequencies. Inducing membrane stresses by clamping the specimen at the ends on this four-point bending set-ups yields larger forces for lower displacements, but the failure always occurs next to the clamps, since that is the location of the highest bending moment.

Clamping the ends of the specimen on a three-point bending set-up, yields almost four times higher bending loads for less than half the displacement when compared with the regular three-point bending set-up. This makes the clamped set-up preferable over the unclamped three-point bending. Fatigue tests have also been performed on the clamped set-up, with good results.

The validation of fatigue damage models might even be done with simple one dimensional beam-theory simulations. Further research must be done on how to avoid the slipping in the grips, since this phenomenon certainly has an influence on the measurement.

ACKNOWLEDGEMENTS

The authors are highly indebted to the university research fund BOF (Bijzonder Onderzoeksfonds UGent) and to Ten Cate Advanced Composites.

REFERENCES

[1] Hansen, U. (1999). Damage development in woven fabric composites during tension-tension fatigue. *Journal of Composite Materials*, **33**(7), 614-639.

[2] Coats, T.W. and Harris, C.E. (1995). Experimental verification of a progressive damage model for IM7/5260 laminates subjected to tension-tension fatigue. *Journal of Composite Materials*, **29**(3), 280-305.

[3] Caprino, G. (2000). Predicting fatigue life of composite laminates subjected to tension-tension fatigue. *Journal of Composite Materials*, **34**(16), 1334-1355.

[4] Gamstedt, E.K. and Sjogren, B.A. (1999). Micromechanisms in tension-compression fatigue of composite laminates containing transverse plies. *Composites Science and Technology*, **59**(2), 167-178.

[5] Rotem, A. (1991). The fatigue behaviour of orthotropic laminates under tension-compression loading. *International Journal of Fatigue*, **13**(3), 209-215.

[6] Sedrakian, A., Ben Zineb, T., Billoet, J.L., Sicot, N. and Lardeur, P. (1997). A numerical model of fatigue behaviour for composite plates: application to a three point bending test. *International Conference on fatigue of composites. 3-5 June 1997, Paris, pp. 415-423.*

[7] Sidoroff, F. and Subagio, B. (1987). Fatigue damage modelling of composite materials from bending tests. *ICCM-VI and ECCM-II: Volume 4. Proceedings, 20-24 July 1987, London, UK, Elsevier, pp. 4.32-4.39.*

[8] Caprino, G. and D'Amore, A. (1998). Flexural fatigue behaviour of random continuous-fibre-reinforced thermoplastic composites. *Composites Science and Technology*, **58**, 957-965.

[9] Van Paepegem, W., De Geyter, K., Vanhooymissen, P. and Degrieck, J. (2006) Effect of friction on the hysteresis loops from three-point bending fatigue tests of fibre-reinforced composites. *Composite Structures*, Volume **72** issue 2, 212-217.

[10] I. De Baere, W. Van Paepegem and J. Degrieck, On the feasibility of a three-point bending set-up for the validation of (fatigue) damage models for thin composite laminates, Accepted for *Polymer Composites*.

[11] I. De Baere, W. Van Paepegem, J. Degrieck, H. Sol , D. Van Hemelrijck and A. Petreli, Comparison of different identification techniques for measurement of quasi-zero Poisson's ratio of fabric reinforced laminates. Accepted for *composites A*

[12] W. C. Young and R. G. Budynas, *Roark's formulas for stress and strain, seventh edition*, ISBN 0-07-121059-8, McGraw-Hill Compaines Inc. 2002